J|A|C|S
ARTICLES
Published on Web 12/07/2006

Anodic Electrodeposition of Highly Oriented Zirconium Phosphate and Polyaniline-Intercalated Zirconium Phosphate Films

Takahiro Takei,*[,†,‡] Yoji Kobayashi,[‡] Hideo Hata,[‡] Yoshinori Yonesaki,[†] Nobuhiro Kumada,[†] Nobukazu Kinomura,[†] and Thomas E. Mallouk[‡]

Contribution from the Center for Crystal Science and Technology, University of Yamanashi, 7 Miyamae, Kofu, Yamanashi 400-8511, Japan, and Department of Chemistry, The Pennsylvania State University, University Park, Pennsylvania 16802

Received August 4, 2006; E-mail: takei@yamanashi.ac.jp

Abstract: Films of highly oriented α-zirconium phosphate and polyaniline-intercalated zirconium phosphate with controllable thickness in the micrometer range were grown anodically on Pt electrodes. To optimize the electrodeposition conditions, the exfoliation of α-zirconium phosphate by tetrabutylammonium (TBA) salts was investigated in several nonaqueous solvents. Acetonitrile was found to be the best solvent for making crack-free, oriented films because of its high vapor pressure, low viscosity, and relatively high permittivity. With TBA salts of neutral or weakly acidic anions (TBACl, TBABr, TBAI, TBA(HSO_4), or TBA(H_2PO_4)), full exfoliation did not occur and α-zirconium phosphate and/or polyaniline were deposited as rough films. With basic anions (TBAF or TBAOH), dense, adherent films were obtained. X-ray diffraction patterns of the films showed that they were highly oriented along the stacking axis. The thickness could be controlled, up to about 40 μm, by limiting the time of the electrodeposition reaction. At monomer concentrations below 1.0×10^{-2} mol/dm^3, the emeraldine form of the intercalated polymer was obtained. Electrodeposition thus provides a thick film alternative to layer-by-layer assembly for intercalation compounds of α-zirconium phosphate with a conducting polymer.

Introduction

Polymer−inorganic hybrids with lamellar structures can be synthesized by intercalation, ion-exchange, and exfoliation. For bulk-phase materials, intercalation and ion-exchange are effective and commonly used techniques.[1−5] Highly oriented films of intercalation compounds can be grown by exfoliation of the layered host material and sequential adsorption of the exfoliated sheets and cationic polymers.[6−10] As a layer-by-layer deposition process, however, this method is limited to thin films (less than about 100 nm). Many applications of hybrid inorganic-conducting polymer films, for example in secondary batteries, antistatic coatings, redox capacitors, and organic solar batteries,[11−17] require thicker films that contain electroactive components such as polypyrrole, polyaniline, or polythiophene. Thicker surface layers and free-standing films of zirconium phosphate[18] and other layered materials[9] have been made by casting suspensions of the exfoliated sheets. While these pellicular films can be intercalated after deposition to give inorganic−organic composites, the method does not offer much flexibility in terms of changing the composition along the stacking axis as the film is grown.

Thick films of inorganic materials can also be deposited electrophoretically. This method was developed for isotropic particles[19−21] and recently has been applied to nanosheets.[22,23] Electrophoretic deposition has several advantages, including electrochemical control of film thickness in the range of micrometers, rapid sequential deposition of materials to make layered

† University of Yamanashi.
‡ The Pennsylvania State University.

(1) (a) Keller, S. W.; Kim, H.-N.; Mallouk, T. E. *J. Am. Chem. Soc.* **1994**, 116, 8817. (b) Kim, H.-N.; Keller, S. W.; Mallouk, T. E. *Chem. Mater.* **1997**, *9*, 1414.
(2) Kaschak, D. M.; Johnson, S. A.; Hooks, D. E.; Kim, H. N.; Ward, M. D.; Mallouk, T. E. *J. Am. Chem. Soc.* **1998**, *120*, 10887.
(3) Takei, T.; Sekijima, K.; Kumada, N.; Kinomura, N. *Solid State Ionics* **2004**, *170*, 111.
(4) Nishimoto, S.; Matsuda, M.; Miyake, M. *J. Solid State Chem.* **2005**, *17*, 811.
(5) Gopalakrishnan, J.; Bhat, V; Raveau, B. *Mater. Res. Bull.* **1987**, *22*, 413.
(6) Kovtyukhova, N. I.; Ollivier, P. J.; Martin, B. R.; Mallouk, T. E.; Chizhik, S. A.; Buzaneva, E. V.; Gorchinskiy, A. D. *Chem. Mater.* **1999**, *11*, 771.
(7) Ram, M. K.; Salerno, M.; Adami, M.; Faraci, P.; Nicolini, C. *Langmuir* **1999**, *15*, 1252.
(8) Wang, L.; Ebina, Y.; Takada, K.; Sasaki, T. *J. Phys. Chem. B* **2004**, *108*, 4283.
(9) Fang, M.; Kim, C. H.; Saupe, G. B.; Kim, H.-N.; Waraksa, C. C.; Miwa, T.; Fujishima, A.; Mallouk, T. E. *Chem. Mater.* **1999**, *11*, 1526.
(10) Sasaki, T.; Ebina, Y.; Tanaka, T.; Harada, M.; Watanabe, M.; Decher, G. *Chem. Mater.* **2001**, *13*, 4661.
(11) Rahmanifar, M. S.; Mousavi, M. F.; Shamsipur, M. *J. Power Sources* **2002**, *110*, 229.
(12) Ryu, K. S.; Hong, Y.-S.; Park, Y. J.; Wu, X.; Kim, K. M.; Lee, Y.-G.; Chang, S. H.; Lee, S. J. *Solid State Ionics* **2004**, *175*, 759.
(13) Martins, C. R.; Paoli, M.-A. D. *Eur. Polym. J.* **2005**, *41*, 2867.
(14) Park, J. H.; Park, O. O. *J. Power Sources* **2002**, *111*, 185.
(15) Takei, T.; Yoshimura, K.; Yonesaki, Y.; Kumada, N.; Kinomura, N. *J. Porous Mater.* **2005**, *12*, 337.
(16) Fusalba, F.; Gouérec, P.; Villers, D.; Bélanger, D. *J. Electrochem. Soc.* **2001**, *148*, A1.
(17) Sivaraman, P.; Hande, V. R.; Mishra, V. S.; Srinivasa Rao, C.; Samui, A. B. *J. Power Sources* **2003**, *124*, 351.
(18) Alberti, G. *Acc. Chem. Res.* **1978**, *11*, 163.
(19) Mondragón-Cortez, P.; Vargas-Gutiérrez, G. *Mater. Lett.* **2004**, *58*, 1336.
(20) Zanetti, S. M.; Varela, J. A.; Leite, E. R.; Longo, E. *J. Eur. Ceram. Soc.* **2004**, *24*, 2445.
(21) Islam, M. A.; Xia, Y.; Telesca, D. A., Jr.; Steigerwald, M. L.; Herman, I. P. *Chem. Mater.* **2004**, *16*, 49.
(22) Sugimoto, W.; Terabayashi, O.; Murakami, Y.; Takasu, Y. *J. Mater. Chem.* **2002**, *12*, 3814.
(23) Koinuma, M.; Seki, H.; Matsumoto, Y. *J. Electroanal. Chem.* **2002**, *531*, 81.

10.1021/ja065677m CCC: $33.50

films, and conformal film growth on curved surfaces. On the other hand, there are some drawbacks to the technique. The deposition is carried out in a wet cell, with charged particles dispersed in a solution that may contain additional electrolyte. Cracking of the film often occurs upon drying. To prevent cracks, the particle size of the dispersed solid and the surface energy of the solvent should both be small in order to relax stresses induced by drying. Nanosheets generally deposit well by electrophoresis because of their small dimensions and high charge density.[22,23]

To grow polymer intercalation compounds as films by the electrophoretic deposition of the nanosheets, one needs a strategy for incorporating the polymer. For conducting polymers, anodic polymerization is a viable strategy because most inorganic nanosheets are negatively charged. The formation of a cationic polymer at the anode should serve to anchor the dispersed sheets to the growing film, because of the low solubility of the intercalation compound in polar organic solvents.

Negatively charged sheets can be obtained from a wide variety of layered compounds, including metal phosphates, layer perovskites, smectite clays, layered titanates, and manganates. In their acidic forms these materials are intercalated and then exfoliated by bases such as propylamine, butylamine, or tetraalkylammonium hydroxides. In this regard, α-zirconium phosphate has been well studied[18,24,25] and was therefore used as the host material in this study. Polyaniline (PAni) has four different states of oxidation and protonation and is an interesting material as the electrode of electrochemical capacitors.[14−17] We therefore studied the preparation of α-zirconium phosphate−PAni hybrid thick films by simultaneous electrophoretic and electrolytic deposition and report the effects of solution composition on the film-growth process and electrochemical properties of the resulting films.

Experimental Section

Preparation of Exfoliated α-Zirconium Phosphate. Several solvents were tested for the electrophoretic and electrolytic deposition reactions. Water, which is ordinarily used as a suspension medium for nanosheets, was studied in preliminary experiments; however, the electrochemical decomposition of water prevented films from forming on the platinum anode. Additionally, because hydrolysis of the α-zirconium phosphate nanosheets is known to occur at ambient temperature, aqueous suspensions are likely to cause some decomposition.[2] Therefore, polar organic solvents (acetonitrile, formamide, nitromethane, ethyleneglycol, acetone, methanol and ethanol) were investigated.

Commercially available α-zirconium phosphate ($Zr(HPO_4)_2{\cdot}H_2O$) powder (IXE-100, TOAGOSEI CO., Ltd.) was suspended in each solvent at a concentration of 6.7×10^{-3} mol/dm^3. Tetrabutylammonium (TBA) salts were added to this suspension at concentrations of $2.5-5.0 \times 10^{-3}$ mol/dm^3. These included basic salts (TBAOH, TBAF) and neutral (TBACl, TBABr, TBAI) and acidic salts ($TBA(HSO_4)$ and $TBA(H_2PO_4)$), as well as equimolar mixtures of TBAOH and TBACl. The solutions were stirred for more than 12 h to exfoliate the α-zirconium phosphate. Aniline was also added to the solution as a monomer for formation of polyaniline (PAni). The aniline/α-zirconium phosphate molar ratio was varied within the range of 0−15.

Electrochemical Deposition. Electrochemical deposition was carried out by using a DC supply (AE-8750, ATTO corp.). Platinum plates (10 mm × 50 mm × 0.1 mm) were used as both electrodes of the two-electrode cell. These Pt plates were immersed vertically in the solution, such that the lower 20 mm was in the solution and the reactive area was 400 mm^2. The separation between the parallel anode and cathode plates was fixed at 10 mm. The electrodeposition experiments were done at constant current, at a current density of 0.01 mA/mm^2. The suspensions were electrolyzed for 15, 30, 60, or 90 min with gentle stirring in order to dislodge any bulk deposits on the electrodes.

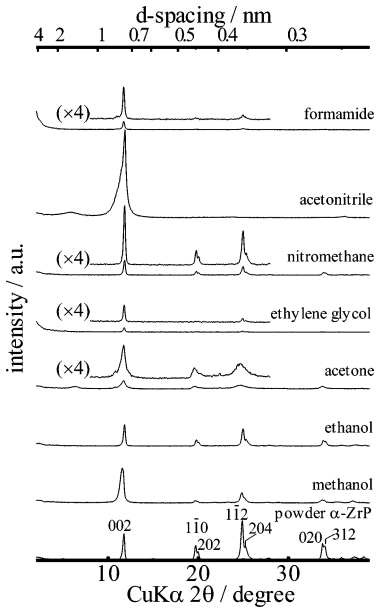

Figure 1. XRD patterns of α-zirconium phosphate films electrophoretically deposited from different organic solvents: α-ZrP concentration = 6.7×10^{-3} mol/dm^3; TBAF concentration = 5.0×10^{-3} mol/dm^3; deposition time = 15 min.

Texture of the Deposited Films. The macroscopic texture of the films was recorded using a digital still camera (S50, Pentax corp.). Film thicknesses and microscale texture were determined by examining the films and their cross sections with an optical microscope (BX60M, Olympus). The microstructure of films was also studied by AFM (NanoScope IIIa, Digital Instruments) and FE-SEM (JSM-6500F, JEOL). X-ray powder diffraction (XRD) patterns were obtained on a Philips Xpert MPD system, operating in $\theta-\theta$ geometry with monochromatized Cu Ka radiation.

The amount of PAni intercalated in the hybrid films was determined by CHN elemental analysis, which was performed by Atlantic Microlab, Norcross, GA. Prior to analysis, volatile components were removed by evacuation for 1 h at ambient temperature. The polymerization of aniline in the hybrid films was confirmed by FT-IR (FTS7000, DIGILAB) with ATR attachment.

Electrochemical Properties. The electrochemical properties of the films were measured by cyclic voltammetry using a potentiostat (BAS100B, BioAnalytical Systems) in a three-electrode cell. Cyclic voltammograms were obtained in acetonitrile/1.0×10^0 mol/dm^3 $NaClO_4$. Two film-covered electrodes and a reference electrode were immersed in the electrolyte solution and cyclic voltammograms were recorded between 0 and 0.8 V vs Ag|AgCl, at sweep rates of 5 and 20 mV/sec.

Results and Discussion

Solvent Choice for the Electrophoretic Deposition of α-Zirconium Phosphate. Figure 1 shows XRD patterns of α-zirconium phosphate films electrodeposited on a Pt anode from several polar organic solvents. Aniline was not added to these solutions, and TBAF was used as the exfoliating base in each case. In all cases, the most intense peak in the pattern corresponds to the 7.6 Å layer spacing of α-zirconium phos-

(24) Ha, B.; Char, K.; Jeon, H. S. *J. Phys. Chem. B* **2005**, *190*, 24434.
(25) Pérez-Reina, F. J.; Olivera-Pastor, P.; Maireles-Torres, P.; Rodríguez-Castellón, E.; Jiménez-López, A. *Langmuir* **1998**, *14*, 4017.

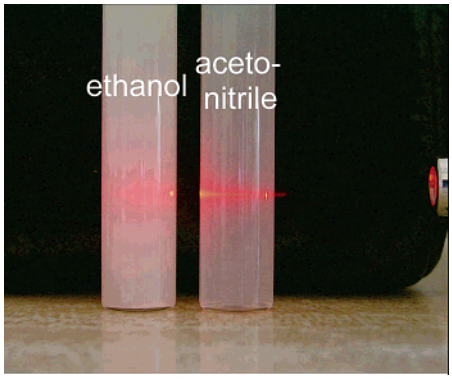

Figure 2. Photograph of the solutions containing α-ZrP, TBAF, and ethanol (left) or acetonitrile (right). The red laser is incident from the right side to demonstrate the Tyndall phenomenon. α-ZrP concentration = 3.3×10^{-3} mol/dm^3; TBAF concentration = 2.5×10^{-3} mol/dm^3.

phate, which is shown at the bottom of the figure for comparison. The relative intensity of this reflection, and the appearance or absence of other reflections in the pattern, can be used as indicators of the degree of preferred orientation and crystallinity of the films, respectively. Films grown from methanol, ethanol, and nitromethane showed relatively narrow lines corresponding to the major reflections of α-zirconium phosphate. This indicates that these films are microcrystalline and are not highly oriented and that full exfoliation did not occur in these solvents. The diffraction patterns of films grown from ethylene glycol and formamide showed weak reflections, consistent with the visual observation that only a small amount of sample deposited on the Pt electrode. We attribute the low yield of electrophoretic deposition in these cases to the higher viscosity of the solvents, which resulted in low mobility of the α-zirconium phosphate sheets. For acetone, the pattern was similarly weak and the diffraction peaks were broadened slightly. It appears that α-zirconium phosphate was not completely exfoliated in acetone; however, the deposited film had a smooth surface and a white color. Because acetone has a low viscosity and high vapor pressure, particulate deposits can dry very well. In contrast, films grown from ethanol or nitromethane had rough surfaces. Films grown from acetonitrile had a qualitatively different XRD pattern, with one intense peak corresponding to the 002 reflection of α-zirconium phosphate and no other distinguishable higher angle lines. This peak is broad and slightly asymmetric toward the low-angle side, as expected for a highly oriented, turbostratically restacked film of exfoliated sheets. The film was translucent and was the firmest of any of the films deposited grown. Relative to the other solvents studied, acetonitrile has a high relative permittivity (37.5), which provides the electrostatic screening needed for complete exfoliation. Its low viscosity and high vapor pressure also favor the formation of highly oriented, crack-free films. Figure 2 shows a photograph of the solutions containing α-zirconium phosphate, TBAF, and ethanol (left) or acetonitrile (right). The red laser was incident from the side to demonstrate the Tyndall phenomenon for only acetonitrile solution. This phenomenon confirms that α-zirconium phosphate was exfoliated in acetonitrile. Acetonitrile was thus used as the solvent in all subsequent experiments.

Exfoliation of α-Zirconium Phosphate by Tetrabutylammonium Salts. Figure 3 shows XRD patterns of α-zirconium phosphate films (again without aniline) electrodeposited from

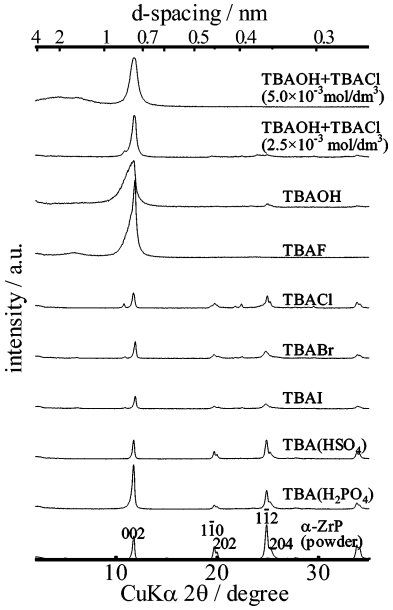

Figure 3. XRD patterns of α-zirconium phosphate films electrophoretically deposited from acetonitrile solution after reaction with neutral and basic TBA salts. α-ZrP concentration = 6.7×10^{-3} mol/dm^3; solvent = acetonitrile; deposition time = 15 min.

acetonitrile solutions containing different TBA salts. In the case of basic anions (F^- or OH^-), a prominent diffraction peak is observed, again implying complete exfoliation and turbostratic restacking of sheets as an oriented film. TBA salts of neutral and acidic anions (Cl^-, Br^-, I^-, HSO_4^-, and $H_2PO_4^-$) gave XRD patterns similar to those obtained of films grown from TBAF in less polar solvents. We can infer from these diffraction patterns that these salts are ineffective exfoliators in acetonitrile and that the films deposited under these conditions consist of randomly oriented microcrystals of α-zirconium phosphate.

Generally, the exfoliation reaction of acidic layered metal phosphates or oxides by basic salts of the TBA^+ cation can be expressed as

$$M{-}OH + TBA^+X^- \leftrightarrow M{-}O^-TBA^+ + HX$$

where M−OH indicates a hydroxyl group on the internal surface of the layered metal solid. TBA^+X^- indicates the tetrabutylammonium salt. Because the driving force for this reaction is formation of HX (i.e., a weak acid or water), X^- must be a basic anion. Since the α-zirconium phosphate can be exfoliated in acetonitrile solutions containing TBAF, it follows that its pK_a is lower than that of HF in this medium. This is consistent with the aqueous pK_a values of H_3PO_4 and HF, which are 2.2. and 3.0, respectively. Films grown from 5.0×10^{-3} mol/dm^3 TBAF, 5.0×10^{-3} mol/dm^3 TBAOH, and 2.5×10^{-3} and 5.0×10^{-3} mol/dm^3 equimolar mixtures of TBAOH and TBACl were translucent, translucent, white and transparent, respectively. It is possible that the HF produced in the first case reacts with some of the exfoliated sheets. For TBAOH, since there were very few electrolytes in the solution, electrodeposition occurred at a faster rate with incomplete orientation. With the equimolar mixtures of TBAOH and TBACl, the α-zirconium phosphate particles were considered from their appearance to be exfoliated completely in the 5.0×10^{-3} mol/dm^3 solution.

Electrodeposition of Hybrid α-Zirconium Phosphate−PAni Films. Next, to study the exfoliation and deposition of

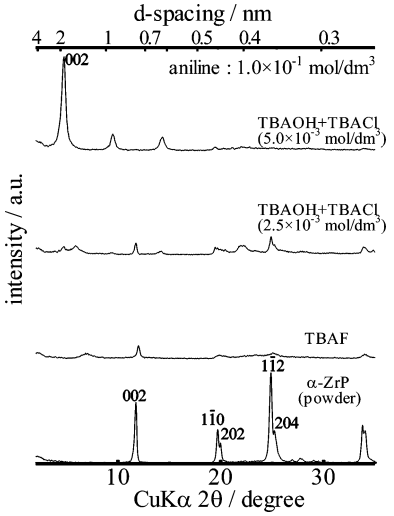

Figure 4. XRD patterns of α-zirconium phosphate/PAni hybrid films grown electrochemically in acetonitrile solution, using different TBA salts. α-ZrP concentration = 6.7×10^{-3} mol/dm^3; aniline concentration = 1.0×10^{-1} mol/dm^3; solvent = acetonitrile; deposition time = 15 min.

α-zirconium phosphate in the presence of aniline monomer, aniline was added to the acetonitrile solutions at a concentration of 1.0×10^{-1} mol/dm^3. Figure 4 shows XRD patterns of films electrodeposited from solutions containing 5.0×10^{-3} mol/dm^3 TBAF and 2.5×10^{-3} and 5.0×10^{-3} mol/dm^3 TBAOH. The film deposited from the TBAF solution was dark brown in color, and only weak diffraction peaks corresponding to residual α-zirconium phosphate and a $d \approx 2.0$ nm intercalated phase were observed in the XRD pattern. Films grown from 2.5×10^{-3} mol/dm^3 TBAOH were white and partially green, and there were also only weak reflections in the XRD pattern. These films contained some cracks formed during drying. In contrast, films grown from 5.0×10^{-3} mol/dm^3 TBAOH showed a progression of layer lines corresponding to a $d = 1.88$ nm intercalated phase. Therefore, monomeric aniline and/or PAni could be intercalated under these conditions. However, because the film was brown, it appears that any polymer formed in the reaction was undoped and some aniline intercalated in the reaction was oxidized.

Since the film color was brown and its surface contained cracks, further optimization of the electrodeposition conditions was carried out. XRD patterns and photographs (Figure 5) show the progression of film structure and color with increasing aniline concentration in the electrodeposition. The lattice spacing increases progressively from 0.76 nm without aniline to 1.14 (~0.4 nm thick polymer layer) and 1.45 (~0.7 nm thick polymer layer) nm at 5.0×10^{-3} and 1.0×10^{-2} mol/dm^3 aniline, respectively. The characteristic green color of emeraldine PAni was observed with 5.0×10^{-3} or 1.0×10^{-2} mol/dm^3 aniline, and the films were adherent and crack-free as shown in Figure 5b. At higher concentrations of aniline (4.0×10^{-2} or 1.0×10^{-1} mol/dm), the films were cracked and their color was gray.

The three phases observed in the XRD patterns correspond to different packing arrangements of PAni between the zirconium phosphate sheets. At low aniline concentration (5.0×10^{-3} mol/dm^3), the predominant phase has a lattice spacing of 1.14 nm, corresponding to a 0.38 nm spacing between the 0.76 nm-thick sheets. This implies that the polymer exists as a monolayer between the sheets with its ring plane parallel to the plane of the sheets. At 1.0×10^{-2} mol/dm^3 aniline, the layer spacing in the film is 1.45 nm, meaning that the polymer occupies a 0.69

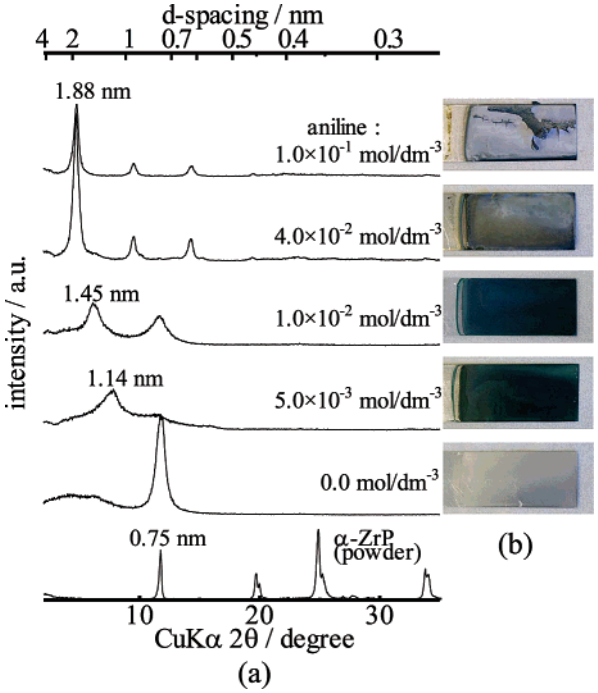

Figure 5. Electrodeposited α-zirconium phosphate/PAni hybrid films as a function of aniline concentration: (a) XRD patterns and (b) photographs. α-ZrP concentration = 6.7×10^{-3} mol/dm^3; TBAOH and TBACl concentration = 5.0×10^{-3} mol/dm^3; solvent = acetonitrile; deposition time = 15 min.

nm high gallery. This spacing is consistent with intercalation of a single PAni layer with the ring plane perpendicular to the plane of the sheet, or a double layer of PAni lying parallel to the sheets. At aniline concentrations of 4.0×10^{-2} and 1.0×10^{-1} mol/dm^3, a layer spacing of 1.88 nm is found, meaning that the polymer or monomeric aniline layer is 1.22 nm thick. This corresponds to a double-perpendicular layer or possibly to other multiple-layer arrangements. In these configurations, full charge compensation of PAni by the adjacent negatively charged sheets is more difficult, and at these high loadings the characteristic green color of the emeraldine salt form of the polymer is not observed. Figure 6 shows FT-IR spectra of the electrodeposited hybrid films with increasing aniline concentration. Absorption bands, ν(N═Q═N), ν(C═C_B), and γ(C—H), attributed to emeraldine PAni were observed in the spectra at 5.0×10^{-3} and 1.0×10^{-2} mol/dm^3 aniline. These bands indicate that emeraldine PAni formed in the films at these concentrations. In the spectra at 4.0×10^{-2} and 1.0×10^{-1} mol/dm^3, absorption bands of aniline, τ(C—H_B) and δ(C—H_B), obviously emerged. This implies that the increase of aniline concentration poses poor polymerization degree.

Elemental analysis (CHN) of the dried electrodeposited films was used to determine the molar ratio n of PAni or monomeric aniline to zirconium phosphate as a function of aniline concentration. Table 1 shows these analytical results. Molar ratios of C/N are around 6.2−7.6 similar to that of aniline or PAni which is 6. These ratios possibly confirm that acetonitrile was removed completely by pretreatment. For TBA^+ cations, Sugimoto et al.[22] have reported that anordically electrodeposited tetratitanate nanosheets do not contain any TBA^+ cations because the TBA^+ cations approach a cathode. We assume that obtained electrodeposited films do not contain any TBA^+ cations.

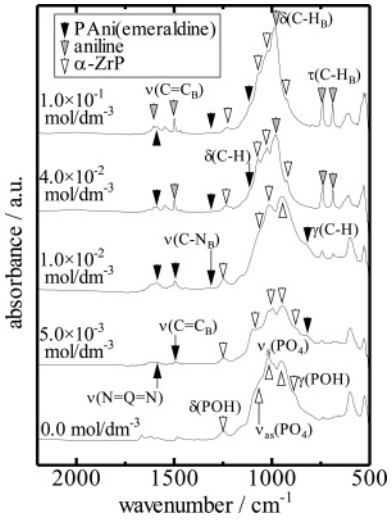

Figure 6. FT-IR spectra of α-zirconium phosphate/PAni hybrid films grown electrochemically in acetonitrile solution as a function of aniline concentration. α-ZrP concentration = 6.7×10^{-3} mol/dm^3; TBAOH and TBACl concentration = 5.0×10^{-3} mol/dm^3; solvent = acetonitrile; deposition time = 15 min.

Table 1. Elemental Composition of Vacuum-Dried PAni/Zirconium Phosphate Electrodeposited Films as a Function of Aniline Concentration

	film composition (wt %)		
aniline concn (mol/dm^3)	C	H	N
0.005	10.0	2.4	1.5
0.010	16.3	2.8	2.6
0.040	27.4	3.5	5.2
0.100	28.1	3.4	5.3
theoretical wt % for $n = 2$	29.7	2.5	5.8

Figure 7 shows that n increases with aniline concentration up to 4.0×10^{-2} mol/dm^3, where a maximum value of about 2 is reached. In the emeraldine salt forms of the intercalation compound (the 1.14 and 1.45 nm phases), n is 0.5−0.9 aniline units per Zr. The volume of the aniline subunit in PAni is about 0.100 nm^3, and the crystallographic area per Zr atom in zirconium phosphate is 0.24 nm^2. If the intercalated phase consisted of polymer only, then $n = 2$ would correspond to a 0.8 nm thick layer of polymer, or a $d \approx 1.56$ nm intercalated phase. However, we observe $d = 1.88$ nm at $n = 2$ and lower values of n for the 1.14 and 1.45 nm phases. This implies that in the as-deposited films, about 75% of the volume in each case

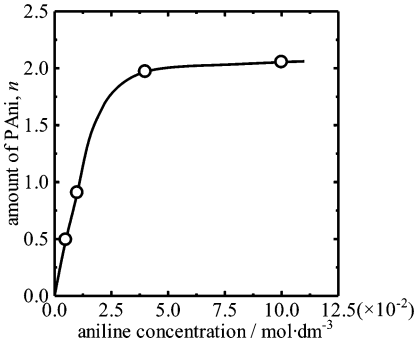

Figure 7. Analytical ratio n of PAni to Zr in hybrid films grown at different aniline concentrations. Films were dried to remove residual solvent and monomeric aniline prior to analysis. α-ZrP concentration = 6.7×10^{-3} mol/dm^3; TBAOH and TBACl concentration = 5.0×10^{-3} mol/dm^3; solvent = acetonitrile; deposition time = 15 min.

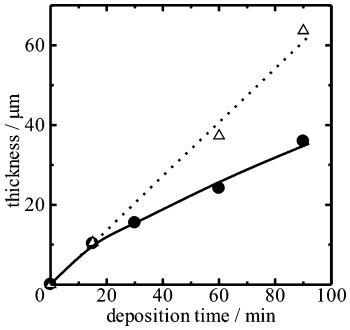

Figure 8. Thickness of electrodeposited α-zirconium phosphate (dotted line) and α-zirconium phosphate/PAni hybrid films (solid line) as a function of deposition time. α-ZrP concentration = 6.7×10^{-3} mol/dm^3; TBAOH and TBACl concentration = 5.0×10^{-3} mol/dm^3; solvent = acetonitrile.

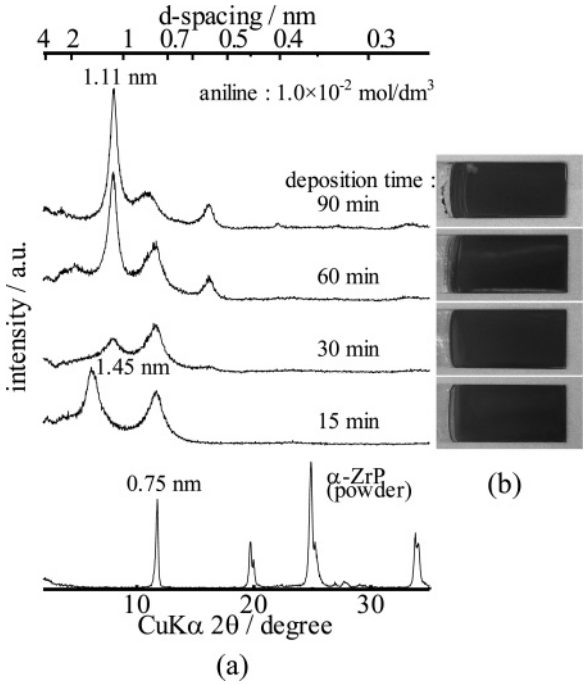

Figure 9. XRD patterns and photographs of α-zirconium phosphate/PAni hybrid films as a function of deposition time: (a) XRD patterns and (b) photographs. α-ZrP concentration = 6.7×10^{-3} mol/dm^3; TBAOH and TBACl concentration = 5.0×10^{-3} mol/dm^3; aniline concentration = 1.0×10^{-2} mol/dm^3; solvent = acetonitrile.

is occupied by the polymer, and the remainder is filled by solvent molecules. The polar solvent molecules likely serve to screen the like charges among the cationic polymer chains in the galleries in the films.

Because only 25−30% of the protons in α-$Zr(HPO_4)\cdot H_2O$ are ionized when the solid is exfoliated with TBA^+OH^{-1}, a 2:1 aniline/Zr ratio (or a 1:1 aniline to phosphate ratio) corresponds to one available proton per 0.70−0.75 aniline unit. The charge density in the emeraldine salt of the polymer is approximately 0.5 per aniline unit, and therefore the sheets contain a sufficiently high loading of protons to charge-compensate the polymer, even at the highest loading observed. As noted above, the reason for incomplete doping of the $d = 1.88$ nm and $n = 2$ phase is most likely steric in origin.

Dependence of Film Thickness on Deposition Time. Figure 8 shows the dependence of the thickness of the film on deposition time. The dotted line shows the thickness of the pure α-zirconium phosphate films, and the solid line shows the

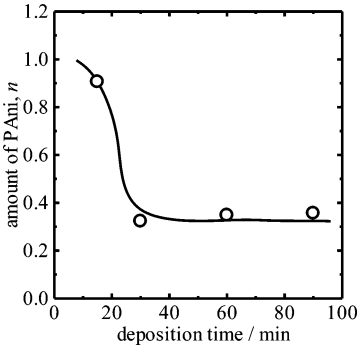

Figure 10. Analytical ratio n of PAni to Zr in hybrid films as a function of deposition time. α-ZrP concentration = 6.7×10^{-3} mol/dm^3; TBAOH and TBACl concentration = 5.0×10^{-3} mol/dm^3; aniline concentration = 1.0×10^{-2} mol/dm^3; solvent = acetonitrile.

PAni/α-zirconium phosphate hybrid films. For the pure α-zirconium phosphate film, the thickness increased linearly and reached more than 60 μm at 90 min. The PAni/zirconium phosphate film grew at a similar rate for about 15 min, and then grew more slowly than the pure α-zirconium phosphate film at longer times. The difference between the deposition rates appears to reflect a difference between purely electrophoretic deposition and mixed electrophoresis/anodic polymerization in the two kinds of films. Possibly because of the increasisng ohmic resistance of the film, at constant current the rate of aniline oxidation decreases relative to the rate of other faradaic processes, such as water oxidation. This should in turn affect the deposition rate and the composition of the films.

Figure 9, parts a and b, shows XRD patterns and photographs of PAni/zirconium phosphate films grown for different periods of time at constant (1.0×10^{-2} mol/dm^3) aniline concentration. The main diffraction peak shifts from 1.45 nm at 15 min to 1.11 nm at times longer than 30 min. The change in the diffraction pattern indicates that the film is becoming richer in zirconium phosphate as the deposition proceeds. Figure 10 confirms that the PAni/Zr ratio n decreases as a function of deposition time. Both the lattice spacing (1.11 nm) and the composition ($n = 0.3$) are consistent with formation of a single layer of PAni with the ring plane parallel to the sheets after long deposition times.

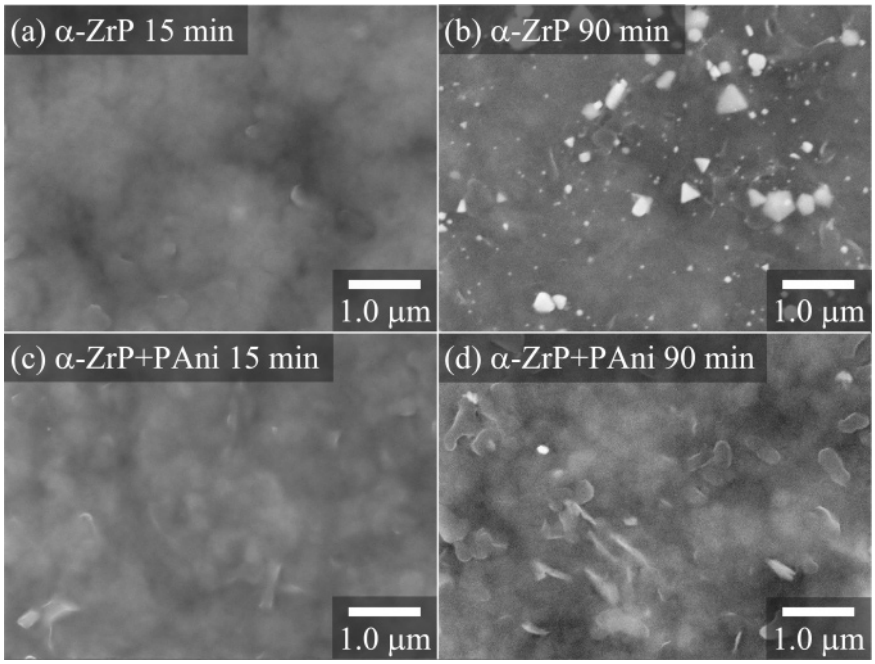

Figure 11. FE-SEM micrographs of electrodeposited α-zirconium phosphate and α-zirconium phosphate/PAni films at 15 and 90 min deposition times.

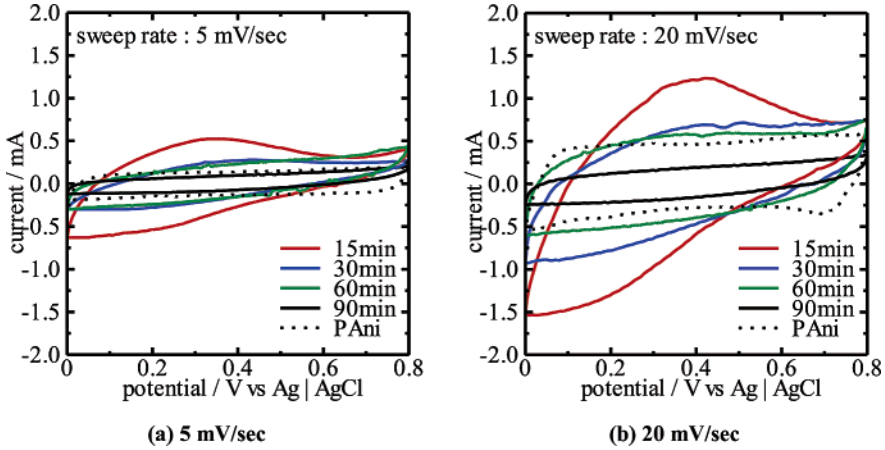

Figure 12. Cyclic voltammetry of α-zirconium phosphate/PAni hybrid films at sweep rates of (a) 5 mV/sec and (b) 20 mV/sec.

Table 2. Electrochemical Capacitances (C_A) in F·g^{-1} of the Hybrid Films

	α-zirconium phosphate + PAni				PAni
	15 min	30 min	60 min	90 min	15 min
sweep rate	EPD	EPD	EPD	EPD	EPD
5 mV/sec	154.1	96.9	54.8	18.0	713
20 mV/sec	85.7	73.3	35.2	9.14	525

Panels a, b, c, and d of Figure 11 show the FE-SEM images of the pure α-zirconium phosphate and PAni/zirconium phosphate films grown for 15 and 90 min, respectively. At short times, the films are relatively smooth, and individual sheets can be seen oriented parallel to the surface. This picture is consistent with the XRD patterns which indicate turbostratically restacked films of strongly preferred orientation. At longer times, there is more evidence of deposition of residual bulk material. Some ridges of approximately 500 nm height can also be observed at longer times, possibly as a result of a decrease in the preferred orientation of the sheets.

Electrochemical Behavior of α-Zirconium Phosphate−PAni Films. Parts a and b of Figure 12 show cyclic voltammograms of the PAni/zirconium phosphate films at sweep rates of 5 and 20 mV/secs, respectively. These films were grown at 1.0×10^{-2} mol/dm^3 aniline concentration, as in Figure 8−11. The general trend is lower electroactivity with increasing deposition time. This result shows the importance of the structure of the intercalated films in mediating charge transport. Despite their greater thickness, films grown at longer times, which contain predominantly the 1.11 nm intercalated phase, have relatively little PAni that is accessible electrochemically. This is most evident in Figure 12a, in which the anodic and cathodic waves at 0.3−0.4 V vs SCE can be clearly seen only for the thinnest films. At the higher scan rate (Figure 12b) the electrochemical response was predominantly non-Faradaic, except for the 15 min film. Table 2 shows the electrochemical capacitances per PAni mass, C_A, derived from the cyclic voltammograms. The maximum C_A of the hybrid films (154 F/g) was obtained at 15 min deposition time. The poor charge transport in the less open 1.11 nm, $n = 0.3$ intercalated phase appears to reduce the capacitance as well as the electrochemical accessibility of intercalated PAni. In addition, the redox reaction of PAni probably requires larger space than that in the 1.11 nm intercalated phase because of geometrical relaxation of PAni which results in a quinoid to benzenoid transition. This suggests that in order to enhance the capacitance of the hybrid films, it is important to adjust the control of the deposition conditions so that the more open 1.45 nm phase is obtained. Unfortunately, all the hybrid films had lower capacitance than pure PAni films grown under similar conditions.

Conclusions

The preparation of layered zirconium phosphate and PAni hybrid films by simultaneous electrophoretic and the electrolytic deposition was demonstrated. After screening a number of polar solvents and exfoliating agents, conditions were found that gave highly oriented, dense films in which the emeraldine salt of the polymer was intercalated between the zirconium phosphate sheets. Acetonitrile was found to be the most effective solvent, most likely because of its high permittivity, low viscosity, and high vapor pressure. Basic tetra-*n*-butylammonium salts (TBAF and TBAOH) were the most effective exfoliating agents. The thickness of films prepared in this way was orders of magnitude greater than those grown by polycation/polyanion layer-by-layer adsorption. Although the concept was not explored here, in principle the electrochemical method also affords some level of control over film composition along the stacking axis. By adjusting the concentration of aniline in the solution phase, different PAni intercalation compounds were grown. The ratio of PAni to α-zirconium phosphate increased from 0.5 to 2.0 or decreased from 0.9 to 0.3 depending on the aniline concentration and the deposition time, respectively.

The hybrid PAni films have a maximum capacitance of about 154 F/g. The capacitance and the fraction of electrochemically accessible PAni in the film appear to be structure dependent, with the more open 1.45 nm intercalation compounds giving better results than the dense 1.11 nm phase. This suggests that higher capacity films might be achieved by pillaring or by other techniques that enhance the transport of ions in the films.

Acknowledgment. This work was supported by University of Yamanashi, by the Grant-in-Aid for Young Scientists Grant (B) 17760543, by the Association for the Progress of New Chemistry, and by the National Science Foundation under Grant CHE-0616450.

JA065677M